JACS
JOURNAL OF THE AMERICAN CHEMICAL SOCIETY

Article

pubs.acs.org/JACS

Phase Boundary Propagation in Large $LiFePO_4$ Single Crystals on Delithiation

Katja Weichert,[†] Wilfried Sigle,[‡] Peter A. van Aken,[‡] Janez Jamnik,[§] Changbao Zhu,[†] Ruhul Amin,[†] Tolga Acartürk,[†] Ulrich Starke,[†] and Joachim Maier*[,†]

[†]Max Planck Institute for Solid State Research, Germany

[‡]Max Planck Institute for Intelligent Systems, Germany

[§]National Institute of Chemistry, Slovenia

Supporting Information

ABSTRACT: Large single crystals of $LiFePO_4$ have been chemically delithiated. The relevance of chemical oxidation in comparison with electrochemical delithiation is discussed. Analyses of the Li content and profiles were done by electron energy loss spectroscopy and secondary ion mass spectrometry. The propagation of the $FePO_4$ phase growing on the surface of the large single crystal was followed by in situ optical microscopy as a function of time. The kinetics were evaluated in terms of linear irreversible thermodynamics and found to be characterized by an induction period followed by parabolic growth behavior of the $FePO_4$ phase indicating transport control. The growth rate was shown to depend on the crystallographic orientation. Scanning electron microscopy images showed cracks and a high porosity of the $FePO_4$ layer due to the significant changes in the molar volumes. The transport was found to be greatly enhanced by the porosity and crack formation and hence greatly enhanced over pure bulk transport, a result which is supposed to be very relevant for battery research if coarse-grained powder is used.

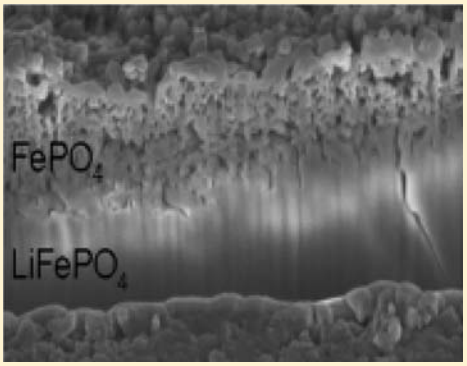

INTRODUCTION

Olivine-type materials have stimulated a lot of research because of their favorable properties for secondary Li batteries.[1] In particular, $LiFePO_4$ was most frequently studied because of its excellent electrode performance, environmental benignity, and low cost.[2] A major difficulty of this material with respect to its use as a cathode in high-performance batteries lies in the poor intrinsic transport properties, which requires the use of fine particles.[3,4] Much of the confusion in the literature concerning transport behavior is simply due to a lack of defect chemical exploration of the bulk phase. Experimentally this became possible when large single crystals of $LiFePO_4$ were grown[5] and analyzed by electrochemical techniques with respect to separating and determining ionic and electronic transport properties as a function of temperature, lithium activity, and doping content.[3,4,6−10]

A similar situation is met in regard to the analysis of the phase transformation kinetics in a $LiFePO_4$ cathode. Different observations have been made and different models proposed.[11−21] The literature reports start with a shrinking core model and its modifications.[1,12,18] Laffont and co-workers reported an inverse shrinking core behavior of platelike $LiFePO_4$ crystals of nanometer range (~200 nm).[15] Here the formation of $FePO_4$ begins in the core of the particle, while the shell consists of $LiFePO_4$ (it should be noted that ref 17ascribes both findings to the same mechanism). There are various recent results showing that the $LiFePO_4/FePO_4$ phase transition is more complex and seems to depend strongly on particle size and morphology. For example, Chen et al.[14] and Ramana et al.[17] observed domain structures of $LiFePO_4$ and $FePO_4$ with crystallites (platelike in the μm range,[14] almost spherical for ~40 nm[17]) after chemical delithiation. Ordering phenomena have recently been observed by transmission electron microscopy (TEM) for electrochemically delithiated $LiFePO_4$ nanowires[22] (diameter ~100 nm half-charged): Li was found to fill every second layer preferentially (*bc* plane, space group *Pnma*).[23] The observation of a digital Li distribution (either fully lithiated or fully delithiated particles) has been addressed in the domino-cascade model[13] (~100 nm particles) and recently in general terms by analyzing the multiparticle equilibrium.[19−21] The complexity of the $LiFePO_4/FePO_4$ phase transition is further increased by size-dependent solubilities.[24−27] For a particle size of 40 nm, a vanishing miscibility gap was reported by Gibot et al.[16]

It must be ascribed to the lack of large enough single crystals that in spite of the enormous interest in the $LiFePO_4/FePO_4$ phase transition, no macroscopic in situ observation of the interface motion has been communicated.

RESULTS AND DISCUSSION

Before we start with the discussion of the results, let us dwell on setting out the meaningfulness of the chemical experiments for interpreting electrochemical delithiation. Electrochemical

Received: August 17, 2011
Published: December 22, 2011

   dx.doi.org/10.1021/ja207124a | *J. Am. Chem.Soc.* 2012, 134, 2988−2992

delithiation of $LiFePO_4$ should be very similar to chemical delithiation as far as the internal mechanism is concerned. As the electron transport in both $LiFePO_4$ and $FePO_4$ is faster than ion transport,[3,4,28] in the arrangement displayed in Figure 1

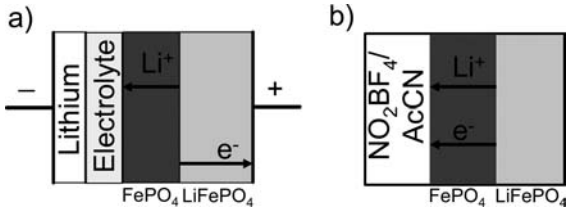

Figure 1. (a) Because of the predominant electronic conductivity in both phases, in the electrochemical experiment (galvanostatic charge), Li^+ is transported through the $FePO_4$ layer while the electron runs toward the positive electrode through the $LiFePO_4$ phase. (b) During chemical delithiation, Li^+ and e^- are transported simultaneously through the $FePO_4$ layer; this process is also determined by ion transport.

it is finally Li^+ transport within $FePO_4$ that determines the delithiation rate of $LiFePO_4$.[29] Naturally, the surface chemistry is different according to different environments, which is only important if the surface reaction step is decisive. The major differences between the two techniques (electrochemical and chemical delithiation) involve the boundary conditions. In the case of a potentiostatic experiment, the Li activity is fixed at the surface, while in a galvanostatic experiment, it is the activity gradient. In the chemical experiment with a large reservoir and quick liquid diffusion, it is the Li activity that is fixed. Hence, the boundary conditions are comparable if the electrochemical process is characterized by a potentiostatic step function.

During the delithiation of large $LiFePO_4$ single crystals, we were able to follow the $FePO_4$ growth as a function of time using optical microscopy to evaluate the kinetics in terms of a growth model. Figure 2 demonstrates the transition of blackish

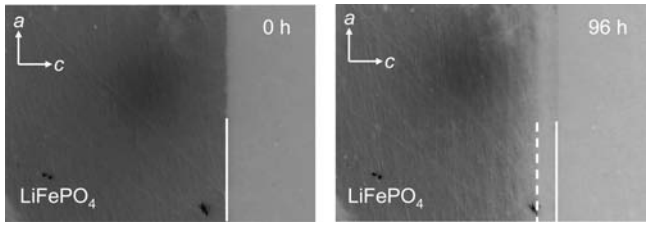

Figure 2. Formation of a transparent $FePO_4$ layer at the surface of the blackish $LiFePO_4$ single crystal after chemical delithiation, as observed by optical microscopy (negatives of the pictures are shown for better contrast). The solid line marks the solid–solution interface and the dashed line the $LiFePO_4$–$FePO_4$ interface. The interface motion could be clearly followed as a function of time.

$LiFePO_4$ into the transparent $FePO_4$ phase after treatment in NO_2BF_4/acetonitrile solution according to the reaction $LiFePO_4 + NO_2BF_4 \rightarrow NO_2 + FePO_4 + LiBF_4$. As shown by powder X-ray diffraction (XRD), the $FePO_4$ layer forms epitaxially (Figure S1 in the Supporting Information). Partial delithiation leads to the formation of an outer shell of $FePO_4$ around the parent $LiFePO_4$ phase, expectedly in agreement with a shrinking core model. (These results are distinctly different for small crystallites, where the $FePO_4$ phase starts growing in the inner part of the particle.[15,30]) Depth profiling of the partially delithiated single crystal was conducted using time-of-flight secondary ion mass spectrometry (TOF-SIMS) which, in agreement with electron energy loss spectroscopy (EELS) results,[30] also confirmed the formation of $FePO_4$ on the surface of the crystal [Figure 3; the phase assignment was done by comparing

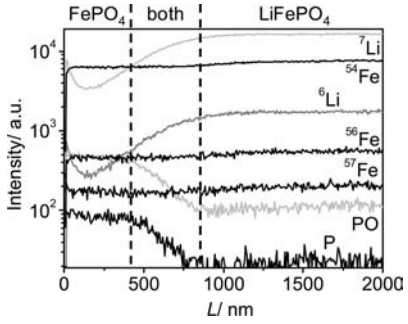

Figure 3. SIMS analysis: depth profile of the partially delithiated $LiFePO_4$ single crystal (investigated area 30 μm × 30 μm, crystal size 2.5 mm × 2.1 mm × 1.3 mm).

the intensity ratios with SIMS data for pure polycrystalline $FePO_4$ (see Figure S2 in the Supporting Information)]. A detailed analysis showed that the apparent width of the effective interfacial zone (~400 nm) is an average width because of the waviness of the interface. When data from a very small area (4 μm*4 μm) were collected, the effective interfacial region was found to be much smaller (~100 nm).

A partially delithiated $LiFePO_4$ single crystal cut by a focused ion beam and investigated by scanning electron microscopy (SEM) showed heavy porosity of the $FePO_4$ layer (Figure 4).

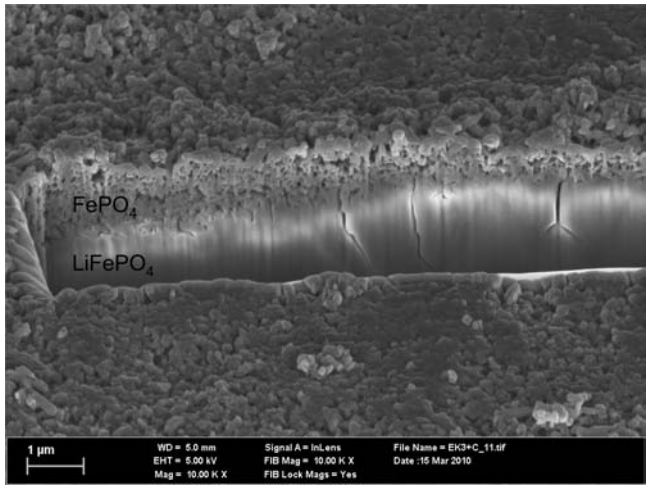

Figure 4. SEM image of a partially delithiated $LiFePO_4$ single crystal. The highly porous $FePO_4$ layer can be seen at the surface of the crystal.

Deep cracks in the micrometer range were found inside the $LiFePO_4$ crystal. Such cracks were also seen in $LiFePO_4$ single crystals exposed to ambient atmosphere and could originate from weathering. Furthermore, the $FePO_4$ layer was not even; its thickness varied from several hundred nanometers up to 1.5 μm.

The growth of the $FePO_4$ layer started after an initial time delay, and the propagation of the phase boundary was followed over a time span of several days. Figure 5 shows a plot of the square of the $FePO_4$ layer thickness L as a function of time.

dx.doi.org/10.1021/ja207124a | J. Am. Chem.Soc. 2012, 134, 2988–2992

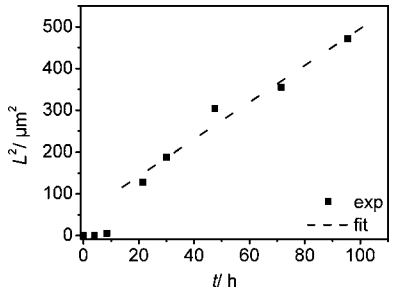

Figure 5. Square of the thickness of the $FePO_4$ layer, L^2, as a function of time, t.

If the very first period is ignored, the behavior is square-root-like (i.e., the plot of L^2 vs t is linear). Such a square-root behavior,

$$L = \sqrt{2\kappa t}$$

is well-known in solid state chemistry and can be derived for transport-controlled phase growth.[31,32] In the following, the observed data will be discussed in terms of different growth models. If one starts from $LiFePO_4$ with the maximum Li deficiency ($Li_{1-\beta}FePO_4$), any further delithiation leads to the formation of $FePO_4$. The growth of the layer is due to Li transport from the outermost $LiFePO_4$ layer through the $FePO_4$ phase that is in contact with the chemical solution. Because Li losses within the $FePO_4$ must be very small, we may assume that any Li transported away from $LiFePO_4$ leads to the formation of $FePO_4$. If we ignore interfacial effects as non-rate-determining, the transport is controlled by steady-state Li transport, that is, ambipolar transport (σ^δ) of Li^+ and e^- through the $FePO_4$ layer:

$$\sigma^\delta = \frac{\sigma_{Li^+}\sigma_{e^-}}{\sigma_{Li^+} + \sigma_{e^-}}$$

If neutral Li defects (which might be present to a large degree[7]) also contribute to the diffusion, a second additive term that is proportional to their diffusivity and concentration must be included.[33]

As shown in the literature,[32] the Li flux density $\mathbf{j}$ is given by

$$\mathbf{j} = -\frac{1}{F^2}\sigma^\delta \nabla\mu_{Li}$$

where $\nabla\mu_{Li}$ is the gradient of the chemical potential of lithium. Alternatively, as $\mathbf{j}$ is locally constant in our quasi-one-dimensional transport problem, it can be expressed as

$$j = -\frac{1}{LF^2}\int \sigma^\delta \, d\mu_{Li} \tag{1}$$

(These equations ignore space charge, which might be of importance for the very initial situations.) The second equation needed is simply the mass-balance expression, which demands that

$$j = \frac{1}{V_m}\frac{dL}{dt} \tag{2}$$

where V_m is the molar volume of $FePO_4$. Combining eqs 1 and 2 yields the following simple differential equation:

$$\frac{dL}{dt} = -\frac{V_m}{F^2}\frac{1}{L}\int \sigma^\delta \, d\mu_{Li} = \frac{\kappa}{L}$$

where

$$\kappa = -\frac{V_m}{F^2}\int \sigma^\delta \, d\mu_{Li}$$

The integration extends from the $LiFePO_4$–$FePO_4$ interface up to the $FePO_4$–solution interface. Even though the minority carrier that determinates σ^δ may sensitively depend on the Li potential, the limits of the integral do not depend on time (the chemical potential at the lower boundary is determined by $Li_{1-y}FePO_4$ and that at the upper boundary by the chemical potential of Li in the solution if local equilibrium applies).

If the growth is interfacially controlled (i.e., if the surface reaction is rate-limiting) the rate dL/dt does not depend on L, so a linear solution follows:

$$L = s\Delta\mu_{Li}t$$

where s is the reaction constant. If both the interfacial reaction and diffusion control are important, we expect the following relation to apply:

$$L = -\frac{\sigma^\delta}{s} + \sqrt{\left(\frac{\sigma^\delta}{s}\right)^2 + 2\sigma^\delta\Delta\mu_{Li}t} \tag{3}$$

with reaction control dominating at low L and transport control at large L (see the Supporting Information).

Figure 5 indicates the curve obtained from the experimental data. Even though the short-time behavior at a first glance might suggest interfacial control, analysis of eq 3 (see the Appendix in the Supporting Information) shows that this is not the case. Equation 3 demands initially a linear behavior in the $L(t)$ representation that later merges into a square-root behavior but without an inflection point. Rather, the behavior in Figure 5 is typical for an induction period. Such an induction period is of course expected, as we do not start out from $Li_{1-\beta}FePO_4$ but from a higher Li content that first needs to be withdrawn at least locally before the phase transformation to $FePO_4$ starts.[24] [As the growth process dominates the kinetics (see Figure 5), we ignore the effect of superimposed Li transport in $LiFePO_4$.] Evaluation of the slopes of the $L^2(t)$ representation yields the effective rate constants κ. For the c axis, the values were found to be 1.3×10^{-12} and 6.2×10^{-12} cm^2/s (on opposite sides of the crystal), and for the a axis, 1.0×10^{-11} cm^2/s was obtained. The statistical error in these data is on the order of $\pm 1 \times 10^{-12}$ cm^2/s. Thus, all of the values are on the order of 10^{-11} to 10^{-12} cm^2/s, with quite some scatter even for the same crystallographic direction. Unexpectedly, the data reveal faster growth of the $FePO_4$ phase along the a direction than along the c axis. This appears to be in contrast to the anisotropy of the chemical diffusion coefficient of lithium found in $LiFePO_4$ single crystals.[4] Here lithium transport is faster in the b and c directions (space group $Pnma$) than in the a direction. The same anisotropy would be expected for Li transport in $FePO_4$ (it should be noted that in the single crystals, differences between the b and c axes are smeared out by antisite disorder[4,34,35]).

For the purpose of a further evaluation, let us for an order of magnitude consideration write κ as

$$\kappa = -\frac{V_m}{F^2}\langle\sigma^\delta\rangle\Delta\mu_{Li}$$

dx.doi.org/10.1021/ja207124a | J. Am. Chem.Soc. 2012, 134, 2988–2992

in which $\langle\sigma^{\delta}\rangle$ is the mean value over the interval $\Delta\mu_{Li}$. Then

$$\kappa = -\frac{V_m}{F^2}\langle\sigma^{\delta}\rangle\left\{[\mu_{Li}(Li_{1-\beta}FePO_4) - \mu^{\circ}_{Li}] - [\mu_{Li}(\text{sink}) - \mu^{\circ}_{Li}]\right\}$$

The difference in μ_{Li} can be expressed by the equilibrium voltage of $Li_{1-\beta}FePO_4$ versus Li and of the value of the chemical solution. The first value is ~3 V, while the second one is unknown but definitely below 10 V [ref 36 gives 5.1 V, while we measured the redox potential under our conditions to be close to 4.2 V (see Figures S3 and S4 in the Supporting Information)]. Obviously, once the initial layer has formed, there is a weak dependence of κ and hence of the rate on the driving force $\Delta\mu_{Li}$ that may be on the order of 1 eV or less (see Figures S3 and S4). The sensitive parameter is the effective transport coefficient. If we conceive $FePO_4$ as being conductive through an excess of Li^+ and e^-,[28] we may anticipate that $\sigma_{Li^+} \ll \sigma_{e^-}$ and hence that $\sigma^{\delta} = \sigma_{Li^+}$. (The detailed investigation in ref 4 gives for $LiFePO_4$ single crystals a ratio of electronic to ionic conductivity of ~10^4. For the conditions under concern, $FePO_4$, the material to which reference is being made, was shown to be predominantly electronic-conducting as well.[28])

From the analyses, we found values of κ between 10^{-12} and 10^{-11} cm^2/s, corresponding to a $\langle\sigma^{\delta}\rangle$ value of 10^{-8} to 10^{-9} S/cm. As the exact expression

$$\kappa = -\frac{V_m}{F^2}\int \sigma^{\delta}\, d\mu_{Li}$$

involves an integration of σ^{δ} over μ_{Li}, it is clear that the mean value will be dominated by the region for which σ_{Li^+} is higher. This will be at the interface with $Li_{1-\beta}FePO_4$, where the Li concentration in $FePO_4$ is highest and the Li carrier content is pretty large.

As pointed out before, the $FePO_4$ layer is not dense but instead is highly porous (Figure 4). This is not surprising at all, since $FePO_4$ has a significantly smaller cell volume than $LiFePO_4$.[1] Therefore, Li removal leads to severe strains in the newly formed $FePO_4$ phase, resulting in breaking of the single-crystallinity followed by penetration of the delithiation agent into the $FePO_4$ layer. As a consequence, Li transport does not take place exclusively within the $FePO_4$ layer but to a great extent involves the liquid in the pores. Here then, the transport of $Li^+BF_4^-$ (the dissolved reaction product of the chemical delithiation) is relevant. The thickness dependence of the growth rate indicates effective diffusion control. If Li^+ ion transport occurs solely through macroscopic pores, a higher κ would be expected (diffusion coefficients of cations and anions in pores are usually in the range of 10^{-5} to 10^{-6} cm^2/s[37]), while pure bulk transport would lead to substantially lower values (κ_b). Hence, it can be concluded that the pore/crack network offers fast diffusion channels but that transport through the bulk parts is not completely dispensable. (The ratio κ_b/κ serves as a rough measure of the volume fraction of this bulk barrier part). Qualitatively similar results were observed by Wood and Wright on nickel–cobalt alloys after oxidation in air.[38] They always observed parabolic growth of the oxide layer, even though it contained cracks and/or pores. They claimed that apart from the direct contact of oxygen with the alloys via the pores, there were still parts of the oxide layer providing a barrier to lattice diffusion and determining the growth rate.

Variability in pore formation could then explain the uneven thickness of the $FePO_4$ layer (Figure 4). More importantly, the unexpected anisotropy found for κ can also be explained if it is the lateral transport from the interior to pores/cracks that limits growth. As transport in the *b* or *c* direction is fastest, growth along the *a* axis[7] (assuming the same anisotropy in $FePO_4$ as in $LiFePO_4$) is quickest.

CONCLUSIONS

Monitoring the propagation of the $FePO_4$ phase formed on large $LiFePO_4$ single crystals upon contact with a delithiation agent has allowed elucidation of the growth kinetics. First, an induction period occurs in which the surface parts of the crystal are depleted of Li up to the composition of coexistence. This induction period is followed by $FePO_4$ film formation. Because of the large variation in molar volume, a porous layer is formed. The kinetics are governed by a parabolic growth law that indicates diffusion limitation. The effective rate constant of parabolic growth amounts to 10^{-11} to 10^{-12} cm^2/s. These effective diffusion coefficients are between those for pure pore and pure solid-state diffusion. This reflects the fact that Li^+ transport occurs over large distances within the pores but that solid-state diffusion through bottleneck parts is still required because of the complex pore microstructure. This is obvious if the pores of relevance do not percolate. If this solid-state diffusion occurs laterally to the growth direction, this then explains the unexpected growth anisotropy. The fact that volume expansion results in microcracking and pore formation, which greatly enhance the kinetics, is clearly of relevance for battery performance. In terms of battery performance using coarse-grained particles, this affects the first conditioning cycles and may stabilize on the nanoscale, as then volume effects can be easily buffered (self-optimization of the microstructure). Indeed, a performance increase on cycling has been observed in various reports (e.g., see ref 39) that in the context of our results can be interpreted as self-optimization of the microstructure. Optimized electrochemical precycling can thus be viewed as a useful and inexpensive method of electrode optimization.

EXPERIMENTAL SECTION

Single crystals of $LiFePO_4$ were grown using the optical floating zone technique. Preparation details and general growth techniques are described in ref 5; the electrical characterization is given in refs 3 and 4. The crystal was cut oriented along the main crystallographic axes, and its size was 2.5 mm × 2.1 mm × 1.3 mm.

For the study of the delithiation kinetics, an Olympus PME3 inverted optical microscope was used. The rectangular single crystal with faces parallel to the major axes of the crystal was placed in a custom-made glass container filled with acetonitrile. Bright-field images of the crystal edges at certain positions were taken. NO_2BF_4 (stoichiometric amounts for ~20% delithiation of the crystal) dissolved in 150 mL of acetonitrile was then added, and images at the same positions of the crystal were taken at different time intervals. Delithiation was performed at room temperature. Profiles of the image intensity were obtained using DigitalMicrograph software (Gatan, Pleasanton, CA) to determine the $LiFePO_4$–$FePO_4$ interface and the $FePO_4$ layer thickness.

SIMS profiles were taken using TOF-SIMS IV from Ion-Tof (primary gun: Ga^+, 15 keV, 1.8 pA, analysis area 30 μm × 30 μm; sputtering gun: O_2^+, 2 keV, 361 nA, sputtering area 200 μm × 200 μm). Only the positive ions were measured by the mass spectrometer.

For powder XRD, a Philips PW 3020 diffractometer and Cu Kα radiation were used.

SEM investigations were performed using a JEOL 6300F field-emission scanning electron microscope (JEOL, Tokyo, Japan)

dx.doi.org/10.1021/ja207124a | J. Am. Chem.Soc. 2012, 134, 2988–2992

operated at 15 keV. The partially delithiated single crystal was cut using a focused ion beam.

■ ASSOCIATED CONTENT

Supporting Information

Appendix containing the detailed growth kinetics model for interfacial reaction and diffusion control, powder XRD data for the partially delithiated $LiFePO_4$ single crystal, SIMS analysis data of polycrystalline $FePO_4$, the redox potential of NO_2BF_4 in acetonitrile, and open-circuit voltage of NO_2BF_4 in acetonitrile after lithiation. This material is available free of charge via the Internet at http://pubs.acs.org.

■ AUTHOR INFORMATION

Corresponding Author

s.weiglein@fkf.mpg.de

■ ACKNOWLEDGMENTS

This paper is dedicated to Professor Hermann Schmalzried on the occasion of his 80th birthday.

■ REFERENCES

(1) Padhi, A. K.; Nanjundaswamy, K. S.; Goodenough, J. B. *J. Electrochem. Soc.* **1997**, *144*, 1188.
(2) Cheruvally, G. *Mater. Sci. Found.* **2008**, *38*, 1.
(3) Amin, R.; Balaya, P.; Maier, J. *Electrochem. Solid-State Lett.* **2007**, *10*, A13.
(4) Amin, R.; Maier, J.; Balaya, P.; Chen, D. P.; Lin, C. T. *Solid State Ionics* **2008**, *179*, 1683.
(5) Chen, D. P.; Maljuk, A.; Lin, C. T. *J. Cryst. Growth* **2005**, *284*, 86.
(6) Amin, R.; Lin, C. T.; Maier, J. *Phys. Chem. Chem. Phys.* **2008**, *10*, 3519.
(7) Maier, J.; Amin, R. *J. Electrochem. Soc.* **2008**, *155*, A339.
(8) Amin, R.; Maier, J. *Solid State Ionics* **2008**, *178*, 1831.
(9) Amin, R.; Lin, C. T.; Maier, J. *Phys. Chem. Chem. Phys.* **2008**, *10*, 3524.
(10) Amin, R.; Lin, C. T.; Peng, J. B.; Weichert, K.; Acarturk, T.; Starke, U.; Maier, J. *Adv. Funct. Mater.* **2009**, *19*, 1697.
(11) Andersson, A. S.; Thomas, J. O. *J. Power Sources* **2001**, *97*−*98*, 498.
(12) Srinivasan, V.; Newman, J. *Electrochem. Solid-State Lett.* **2006**, *9*, A110.
(13) Delmas, C.; Maccario, M.; Croguennec, L.; Le Cras, F.; Weill, F. *Nat. Mater.* **2008**, *7*, 665.
(14) Chen, G. Y.; Song, X. Y.; Richardson, T. J. *Electrochem. Solid-State Lett.* **2006**, *9*, A295.
(15) Laffont, L.; Delacourt, C.; Gibot, P.; Wu, M. Y.; Kooyman, P.; Masquelier, C.; Tarascon, J. M. *Chem. Mater.* **2006**, *18*, 5520.
(16) Gibot, P.; Casas-Cabanas, M.; Laffont, L.; Levasseur, S.; Carlach, P.; Hamelet, S.; Tarascon, J. M.; Masquelier, C. *Nat. Mater.* **2008**, *7*, 741.
(17) Ramana, C. V.; Mauger, A.; Gendron, F.; Julien, C. M.; Zaghib, K. *J. Power Sources* **2009**, *187*, 555.
(18) Andersson, A. S.; Kalska, B.; Häggström, L.; Thomas, J. O. *Solid State Ionics* **2000**, *130*, 41.
(19) Dreyer, W.; Jamnik, J.; Guhlke, C.; Huth, R.; Moskon, J.; Gaberscek, M. *Nat. Mater.* **2010**, *9*, 448.
(20) Ceder, G.; Malitz, R. Presented at the 15th International Meeting on Lithium Batteries (IMLB 15), Montreal, Canada, 2010; abstract 327.
(21) Burch, D.; Singh, G.; Ceder, G.; Bazant, M. *Diffus. Defect Data, Part B* **2008**, *139*, 95.
(22) Zhu, C.; Yu, Y.; Gu, L.; Weichert, K.; Maier, J. *Angew. Chem., Int. Ed.* **2011**, *50*, 6278.
(23) Gu, L.; Zhu, C.; Li, H.; Yu, Y.; Li, C.; Tsukimoto, S.; Maier, J.; Ikuhara, Y. *J. Am. Chem. Soc.* **2011**, *133*, 4661.
(24) Yamada, A.; Koizumi, H.; Nishimura, S. I.; Sonoyama, N.; Kanno, R.; Yonemura, M.; Nakamura, T.; Kobayashi, Y. *Nat. Mater.* **2006**, *5*, 357.
(25) Meethong, N.; Huang, H. Y. S.; Carter, W. C.; Chiang, Y. M. *Electrochem. Solid-State Lett.* **2007**, *10*, A134.
(26) Kobayashi, G.; Nishimura, S. I.; Park, M. S.; Kanno, R.; Yashima, M.; Ida, T.; Yamada, A. *Adv. Funct. Mater.* **2009**, *19*, 395.
(27) Wagemaker, M.; Singh, D. P.; Borghols, W. J.; Lafont, U.; Mulder, F. M.; Badi, S. P.; Kan, W. H.; Ellis, B.; Nazar, L. F. Presented at the 2010 MRS Fall Meeting, Boston, MA, 2010; abstract KK 1.9.
(28) Zhu, C.; Weichert, K.; Maier, J. *Adv. Funct. Mater.* **2011**, *21*, 1917.
(29) In the chemical experiment, electrons and ions are supplied at the same boundary. This cannot be simply mimicked in an electrochemical experiment, as then electrodes would have to be supplied at the liquid−solid interface. However, as electronic transport is fast, this is not necessary. On the other hand, an electrochemical storage experiment on the single crystal with liquid and electrode phases of different size would not be feasible because of the large diffusion length.
(30) Sigle, W.; Amin, R.; Weichert, K.; van Aken, P. A.; Maier, J. *Electrochem. Solid-State Lett.* **2009**, *12*, A151.
(31) (a) Tammann, G. *Z. Anorg. Allg. Chem.* **1920**, *111*, 78. (b) Wagner, C. *J. Electrochem. Soc.* **1956**, *103*, 571.
(32) Schmalzried, H. *Solid State Reactions*; VCH: Weinheim, Germany, 1981; pp 170−180.
(33) Maier, J. *J. Am. Ceram. Soc.* **1993**, *76*, 1212.
(34) Malik, R.; Burch, D.; Bazant, M.; Ceder, G. *Nano Lett.* **2010**, *10*, 4123.
(35) Adams, S.; Rao, R. P. *Solid State Ionics* **2011**, *184*, 57.
(36) Yamada, A.; Chung, S.-C. *J. Electrochem. Soc.* **2001**, *148*, A960.
(37) *Theory and Applications of Transport in Porous Media*; Bear, J., Ed.; Springer: Berlin, 1986; Vol. *1*.
(38) Wright, I. G.; Wood, G. C. *Oxid. Met.* **1977**, *11*, 163.
(39) Zhang, S. S.; Allen, J. L.; Xu, K.; Jow, T. R. *J. Power Sources* **2005**, *147*, 234.